INNOVATIVE AND OPTIMAL DESIGN OF MAGNETIC CIRCUIT OF IDLER IN BELT CONVEYOR

Rui XUE[1]

In recent years, China's mining industry has made remarkable achievements in technological innovation, driving the entire mining industry to flourish. With the deep mining of underground mineral resources, the traditional simple mechanical transport mode can not meet the complex and changeable work needs. Therefore, in order to adapt to the harsh environment of mine operation, it is imperative to upgrade the technology of the existing belt conveyor.A new type of multi-stage coil magnetorheological damper roller is developed to solve the problems of too fast speed and out of control in downward transportation of belt conveyor. This kind of damping roller is designed skillfully, which not only retains the structural characteristics of the traditional damping roller, but also improves the performance significantly through innovative technology. The core of the system is to place several coils in a fixed magnetic loop in parallel, which greatly enhances the magnetic field strength and optimizes the distribution uniformity of the magnetic field.During the research and development process, the technical team carried out in-depth theoretical research on the magnetic circuit of the damping roller, and established an accurate mathematical model of damping torque. At the same time, they also used advanced genetic algorithm to optimize the design parameters to determine the optimal geometric structure of the damping roller.The research results not only provide valuable theoretical basis and practical guidance for the braking system of belt conveyor, but also can improve the working efficiency and safety performance of belt conveyor. In the long run, this will promote the overall improvement of China's mine production efficiency and inject new vitality for the sustainable development of mining industry.

Keywords: Belt conveyor, Damp torque, Magnetic Field Strength, Excitation Coil

1. Introduction

The existing lower belt conveyors are extremely prone to mistracking and slipping during operation, which in turn leads to safety production accidents [1]. In order to avoid such accidents, the lower belt conveyor generally needs to have additional braking devices to automatically control the speed of the conveyor [2,3]. At present, the frictional braking of the lower belt conveyor mainly includes damper plate brake and damper roller brake [4,5]. Damper plate braking relies on the sliding friction between the damper plate and the conveyor belt [6], but the wear on the conveyor belt is serious [7]. The conveyor belt uses oil bearing to

[1] Prof., Shandong Vocational College of Science and Technology, Weifang, Shandong 261053, China, e-mail: xuerui126@126.com.

increase the running resistance of the roller for braking, but the damping force is limited [8,9]. In order to solve the deficiency of traditional magnetorheological damper in damping torque, and to deal with the overspeed and even stall risk of downward belt conveyor caused by traditional friction brake, we have innovatively designed a multi-stage coil magnet rheologic damping drum, which is perfectly compatible with the traditional undamped drum structure. The magnetic field intensity of magnetorheological fluid in the working gap is enhanced and the distribution uniformity of the magnetic field is optimized. Based on the analysis of magnetic circuit theory, the mathematical model of damping moment is established. In this study, the effect of the number of excitation coils on the damping clearance magnetic induction is investigated, and the combined effect of the number of excitation coils and the belt speed on the output damping torque is analyzed. In order to further optimize the performance of the damping drum, we use genetic algorithm, a powerful optimization tool. By means of genetic algorithm, we determine the optimal geometric parameters of the damping roller to ensure that it can achieve the best working state in practical application. This innovative design not only improves the safety and stability of the belt conveyor, but also provides a new technical support for the sustainable development and efficiency improvement of the mining industry.

2. Material and methods

The design of the common roller with a roller diameter of 108 mm and a roller length of 465 mm was selected [10]. The structure and main geometric parameters of the designed magnetorheological damper roller are shown in Fig. 1. D0, D1, D2, D3 are the diameter of the idler shaft, the outer diameter of the stationary magnetic guide ring, the inner diameter of the rotating magnetic cylinder, and the outer diameter of the rotating magnetic cylinder. C and h are the length and thickness of the exciting coil respectively. L1 is the length of the damping gap between adjacent excitation coils, and d the thickness of the damping gap. The rotating magnetic tube is embedded in the inside of the roller through an interference connection [11,12]. The rotating magnetic plate on the left and right sides and the rotating magnetic tube are fixed by bolts [13]. The recess of the stationary magnetically permeable ring has several exciting coils connected to the idler shaft by an interference connection [14,15]. A magnetorheological fluid is filled in the space between the stationary magnetic conducting ring and the rotating magnetic conducting cylinder r [16,17].

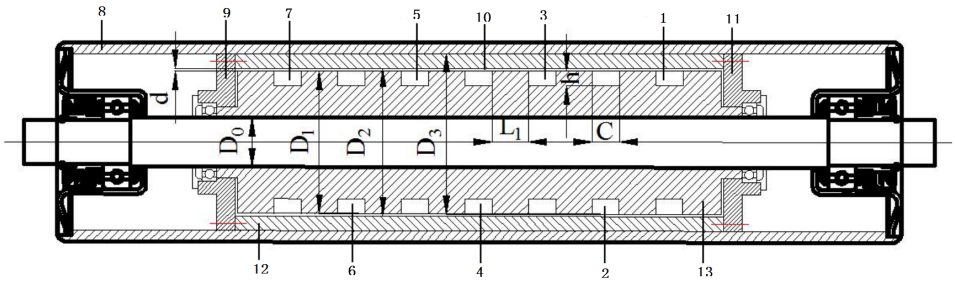

Fig. 1 Geometric structure and parameters of magnetorheological fluid braking and damping roller

When no excitation current is passed through the exciting coil, the viscous resistance generated by the magnetorheological fluid is small. The magnetorheological damper idler can be used as a conventional undamped idler. When the excitation coil is energized, the viscosity of the magnetorheological fluid increases several orders instantaneously, which in turn produces a damping torque that prevents the belt conveyor from stalling or even overspeed during the lowering process. By controlling the magnetic field current and the length of the rotating cylinder, we can control the damping torque flexibly. Compared with the traditional shear-type damper, this new type of damper drum has been greatly improved in design. It employs multiple coils placed in parallel over the magnetorheological fluid work area, thus significantly enhancing the magnetic induction of the area and optimizing the uniform distribution of the magnetic field. This innovative design not only improves the performance of the damper, but also provides a more reliable guarantee for the stable operation of belt conveyor and other equipment.

The damping torque generated by magnetorheological damper is mainly dependent on the exquisite design of its magnetic circuit under the condition of specific excitation current and the length of rotating magnetic cylinder. This design is essential to optimize the performance of the damper, which ensures that the magnetorheological fluid can respond effectively to changes in the magnetic field in the operating region, thus generating the required damping torque, provide the key support for the stable operation of the equipment. Therefore, in order to make full use of the rheological effect of the magnetorheological fluid, the produced damping torque is increased as much as possible while the cost-effectiveness is also being taken into account. Both the rotating magnetic tube and the static magnetic conducting ring are made of DTE4 electromagnetic pure iron with excellent magnetic permeability and demagnetization performance, and the magnetic fluid is MRF132DG. When the excitation coil is energized, the rotating magnetic flux, the magnetorheological fluid and the stationary magnetic cylinder form a magnetic path, and the equivalent magnetic circuit is shown in Fig. 2.

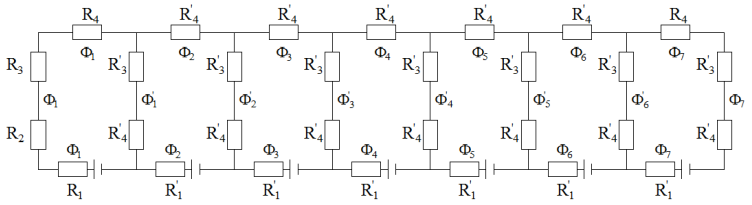

Fig. 2 Magnetic circuit model of magnetorheological fluid braking and damping roller

In the figure, R1, R2, R3, and R4 are the reluctances of the stationary magnetic flux rings at the two ends of the damper idler, respectively, and R1', R2', R3', and R4' correspond to the reluctance of the common portions of the two exciting coils, respectively. Φ1-Φ7, Φ1'-Φ6' indicate the magnetic flux of each part of the magnetic circuit respectively, which is determined by Ampere's law [18]:

$$\phi_i' = \phi_i + \phi_{i+1} \text{ ,i=1,2,3,4,5,6} \tag{1}$$

$$N_1 I_1 = (R_1 + R_2 + R_3 + R_4)\phi_1 + (R_2' + R_3')\phi_1' \tag{2}$$

$$N_i I_i = R_1'\phi_i + (R_2' + R_3')(\phi_{i-1}' + \phi_i') + R_4'\phi_i' \text{ ,i=2,3,4,5,6} \tag{3}$$

$$N_7 I_7 = (R_1 + R_2 + R_3 + R_4)\phi_1 + (R_2' + R_3')\phi_1' \tag{4}$$

From the basic theory of magnetic circuits, the reluctance of the annular axial unit is:

$$R_c = \frac{l}{\pi\mu_0\mu(r_2^{\,2} - r_1^{\,2})} \tag{5}$$

The reluctance of the annular radial unit is:

$$R_a = \frac{1}{2\pi p\mu_0\mu}\ln\frac{r_2}{r_1} \tag{6}$$

Where l is the length of the annular axial unit, μ0 and μ are vacuum permeability and material permeability, respectively. r1 and r2 are the outer diameter and inner diameter of the annular unit, respectively. p is the width of the annular radial unit. From this, the magnetic reluctance of each part in Fig. 2 can be calculated. Through the magnetic circuit design, the initial design geometry parameters of the magnetorheological damper roller are shown in Table 1.

Table 1

The main structural parameters of magnetorheological fluid braking and damping roller

Parameter	Size/mm
Roller shaft diameter D0	26
Rotary magnetic cylinder inner diameter D2	72
Rotating magnetic tube outer diameter D3	96
Static magnetically conductive ring outer diameter D1	70
Excitation coil width C	12
Excitation coil thickness h	6
Magnetorheological fluid damping gap d	1
Length of magnetorheological fluid region between adjacent coils L1	22.5

The shear thinning of magnetorheological fluid during shearing and the influence of magnetic field strength on yield stress are two problems we should consider. The Herscher-Bulkley model is used to characterize the properties of magnetorheological fluid:

$$\tau = \tau_y(H) + K(H)(\frac{\omega D_1}{2d})^{n(H)} \tag{7}$$

In the formula, τ is the shear stress of the magnetorheological fluid; τy(H),K(H),n(H) are the magnetic yield stress, viscosity, and flow coefficient of the magnetorheological fluid, respectively. H is the magnetic field strength in the working gap of the magnetorheological fluid, ω is the rotational angular velocity of the damper roller. The shearing moment between the stationary magnetically permeable ring and the magnetorheological fluid is:

$$T_C = \tau \bullet 2\pi(\frac{D_1}{2})^2 L \tag{8}$$

Because the magnetic field intensity distribution in the magnetorheological damping gap is not uniform, the damping gap is divided into N points, and the magnetic field between the adjacent two points is approximately uniform, then the equation (7) is substituted into equation (8).

$$T_C = \frac{D_1}{2}^2 \pi\sum_i^N (L_{i+1} - L_i)(\tau_y(\frac{H_{i+1} + H_i}{2}) + K(\frac{H_{i+1} + H_i}{2})(\frac{\omega D_1}{2d})^{n(\frac{H_{i+1}+H_i}{2})}) \tag{9}$$

In the formula: L is the length of the stationary magnetically permeable ring. When the magnetic field strength H is zero, the viscous damping torque T0 of the magnetorheological damper idler under zero magnetic field conditions can be obtained.

3. Discussion

As a new type of braking technology, magnetorheological fluid brake has the advantages of low energy consumption [19], adjustable and controllable damping force [20], and easy integration of other new control technologies [21], which can make up for the traditional damper plate brake and the disadvantage of traditional damper roller braking. However, the damping force provided by the conventional rotary magnetorheological damper device is still very limited. In order to further improve the damping force, Nam TH [22], Yu J [23], Nguyen [24], etc., by changing the shape of the rotor or stator, and Choi [25], Wu J [26], etc., by changing the shape of the exciting coil and Arrangement type, Chen Deming [27], Wang [28], etc. increase the damping torque of the output by increasing the number of stators. However, these methods make the structure and

assembly process of the magnetorheological device more complicated, and it is difficult to process it into a form of roller.

3.1 Magnetorheological damping roller magnetic path

After defining the core structure parameters of the damper roll, we can adjust the damping torque of the damper roll accurately by means of exciting current regulation and linear control. When designing the structure, the influence of the number of coils and the length of the stationary magnetically permeable ring on the output damping torque should be considered. We design according to the traditional non-damping idler roller, the designed magnetorheological damping idler roller diameter is 108mm.In order to facilitate manufacturing and assembly, the static magnetic ring and the excitation coil length are kept unchanged during design. Then the influence of the number of excitation coils on the magnetic field and output damping torque of the magnetorheological damping roller is studied.

Since the damper roller roll and the rotating magnetic plates on the left and right sides of the stationary magnetically permeable ring are not magnetically permeable, the model needs to be simplified during analysis, and only the inner magnetically permeable portion of the damper roller is selected for research. When the number of excitation coils is set from 1 to 7, through the detailed finite element analysis and measurement of the damper drum, we have successfully obtained the magnetic field distribution. Under the conditions of setting the number of excitation coils as 1,3,5 and 7 respectively, the corresponding magnetic field lines and magnetic induction distributions are obtained, as shown in Fig. 3.

It can be seen from Fig. 3, when the adjacent exciting coils are connected to the opposite current, the magnetic lines of force are centered on each of the exciting coils and vertically pass through the magnetorheological fluid damping gap between the adjacent coils to form a closed loop. The maximum magnetic induction intensity appears at the left and right ends of the coil and its corresponding magnetorheological fluid damping gap, and its value is almost equal, which is less than the saturation magnetic induction intensity of DT4E electromagnetic pure-iron, which can meet the design requirements.

In order to more intuitively analyse the distribution of the magnetic induction intensity in the entire magnetorheological fluid damping gap, when the number of excitation coils is 1, 3, 5, 7, respectively, the magnetic induction intensity in the magnetorheological fluid damping gap along the static magnetically conductive ring was studied. The distribution in the radial length is shown in Fig. 4.

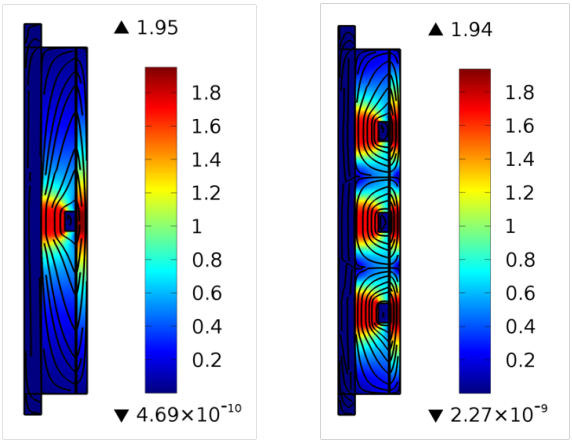

(1) 1 excitation coil (2) 3 excitation coils

(3) 5 excitation coils (4) 7 excitation coils

Fig. 3 Distribution of magnetic flux density of magnetorheological fluid braking and damping roller

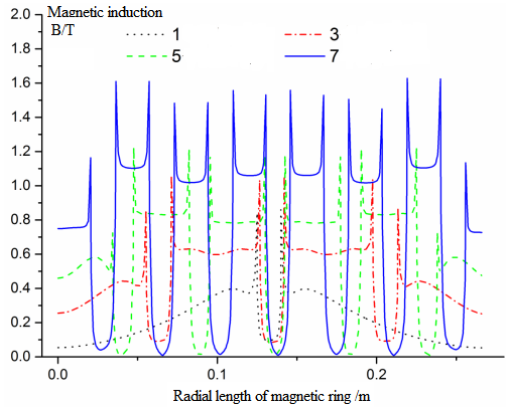

Fig. 4 Distribution of magnetic flux density along static magnetic conduction ring radial path in damping gap

Looking at Fig. 4, we can see that the region directly corresponding to the excitation coil in the magnetorheological fluid damping gap has almost zero

magnetic induction, and this phenomenon is independent of the number of excitation coils. When there is only one excitation coil, the magnetic induction in the magnetorheological damping gap on the left and right side of the coil increases along the radial direction of the stationary magnetic conducting ring, but the strength decreases with the distance. This is mainly due to the long radial size of the fixed conductance ring and the relatively limited magnetic field influence range produced by a single excitation coil. However, as the number of excitation coils increases to 3, 5, and 7, it becomes apparent that the magnetic induction in the damping gap between adjacent coils become very close. As the number of excitation coils increases, the magnetic induction fluctuation in the damping gap decreases, while the overall value increases. This is because the magnetic fields generated by adjacent coils are superimposed on each other, thus significantly improving the magnetic field strength and uniformity. This discovery is of great significance for optimizing the design of magnetorheological dampers and improving their performance in practical applications.

Meanwhile, when the number of excitation coils is increased to 7, the average magnetic induction of magnetorheological fluid between adjacent coils reaches 1.08 t, which is slightly higher than the saturation magnetic induction of magnetorheological fluid. Therefore, the number of excitation coils can not be increased without limitation while the excitation current remains constant. For the 180mm diameter magnetorheological damper drum we studied, the maximum number of excitation coils was determined to be 7, which is the key limiting factor to achieve the optimal damping effect under these conditions.

3.2 Factors affecting damping torque

3.2.1 Influence of the number of excitation coils on damping torque

After further analysis, we found that as the number of excitation windings increases, the magnetic induction between adjacent excitation windings not only increases, but also becomes more uniform. Nevertheless, the actual length of the effective damping gap is reduced by the fact that the damping gap magnetic induction at the excitation coil location is almost zero. At the same time, magnetorheological fluid itself will gradually enter the state of magnetic saturation. Therefore, we can not increase the number of excitation coils indefinitely. In fact, as the number of excitation coils increases from 1 to 7, the output damping torque of the damper changes, as shown in Fig. 5.

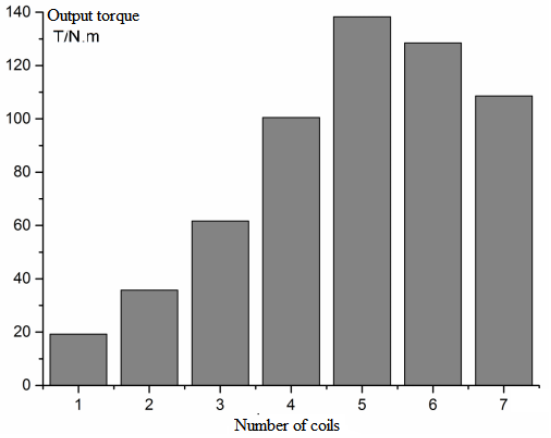

Fig. 5 The relationship between the number of excitation coils and output damping moment

Looking at Fig. 5, we can conclude that the simulation results are consistent with the previous theoretical analysis. When the number of excitation coils of magnetorheological damper increases from 1 to 5, the output damping torque of the damper shows an increasing trend, that is, with the increase of the number of excitation coils, the damping moment increases gradually. However, when the number of excitation winding increased from 5 to 7, the output damping torque began to decrease with the increase of the number of excitation winding. Thus, the optimum number of excitation coils is five. Under this configuration, the magnetorheological damper roller can reach its maximum output damping torque of 138 N.m.

3.2.2 Influence of belt speed on output damping torque

The belt conveyor belt speed is different. The damping torque required is also different for preventing stall or overspeed. When the belt speed is 1.0, 1.25, 1.6, 2.0, 2.5, 3.15 m/s, the magnetorheological damping damper torque of the roller output is shown in Fig. 6.

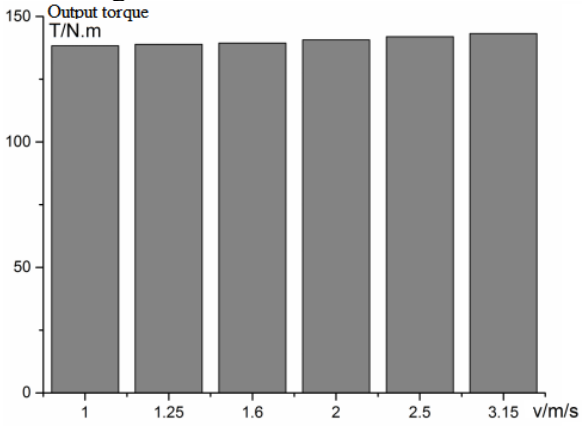

Fig. 6 The relationship between the belt velocity and output damping moment

It can be clearly observed from the relevant charts that with the increase of the speed of the belt conveyor, the output damping torque of the magnetorheological damping roller is stable without obvious fluctuation. This shows that the change of belt speed has a limited influence on the damping torque produced by the magnetorheological damper roll, which can be almost ignored.

4. Results

After determining the optimal number of excitation coils, the geometrical parameters of the magnetorheological damper idler need to be further determined to maximize the damping torque output under the action of the magnetic field. Therefore, the optimized objective function can be expressed as:

$$f_1(x) = \frac{1}{T_c(x)} \tag{10}$$

Where x is the design variable of the magnetorheological damper idler. During optimization, the length of the magnetorheological damping gap between any two adjacent excitation coils is kept equal. At the same time, the design variable x=(D1 , h , C) can be determined by the structural parameters of the traditional undamped roller. The range of the design variable x is shown in Table 2.

Table 2

The upper and lower bounds of design variables

Design variable x	X min	X max
Outer diameter of stationary magnetic ring D1 / mm	50	92
Excitation coil thickness h / mm	4	12
Excitation coil width C / mm	10	25

On one hand, the design variables need to be limited by the geometry parameters of the magnetorheological damper idler. On the other hand, the magnetorheological fluid in the damping gap and the magnetic field strength of the yoke material cannot reach a saturated state. The constraints of the resulting optimization model are:

$$\begin{cases} D_0 + 2h < D \\ D_2 = D_1 + 2d \\ 5C < L \\ B_{1\max} \le 0.95T \\ B_{2\max} \le 2.1T \end{cases} \tag{11}$$

In the formula, B1 max is the maximum magnetic induction in the damping gap. B2 max is the maximum magnetic induction of the yoke material.

By studying Gregor Mendel's theory of genetics and Darwin's theory of evolution, an efficient global search algorithm that mimics biological evolution has become the genetic algorithm of today [29] . The genetic algorithm can

control the whole process adaptively and obtain the optimal solution of the problem. The optimum design of magnetic circuit parameters of magnetorheological damping roller includes optimization variables, constraint conditions and objective functions. The air gap distance, the length of lower yoke, the height of upper yoke and lower yoke and the middle height of Magnetic Bowl were selected as the optimization variables, the objective of the optimization is to improve the internal magnetic induction of the damping gap, and the second-order polynomial response surface model is taken as the objective function [30].The genetic algorithm is used to optimize the objective function. The optimization process is shown in Fig. 7.

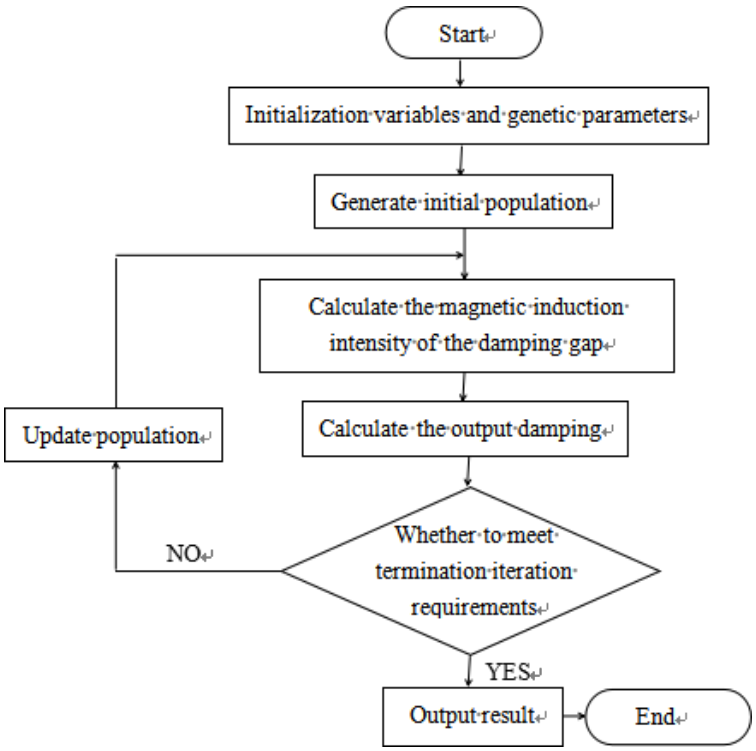

Fig. 7 Flow chart of magnetorheological fluid braking and damping roller

After 308 iterations, the values of the optimized design variables are: D1=78mm, h=8mm, C=15mm. The distribution of the magnetic induction intensity in the damping gap before and after optimization along the radial length of the stationary magnetically permeable ring is shown in Fig. 8.

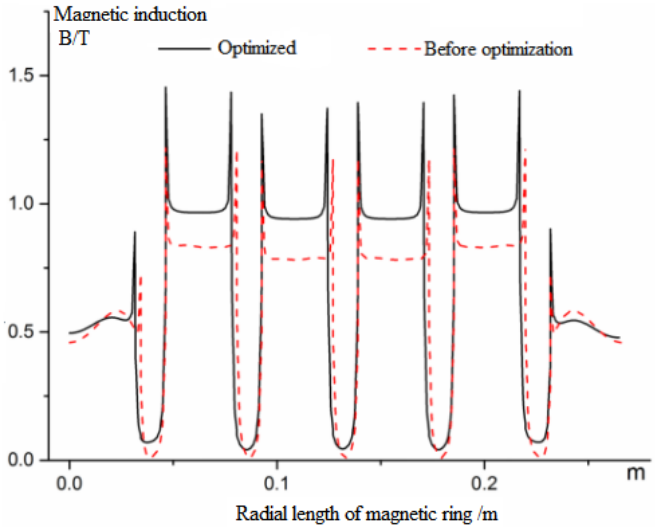

Fig. 8 Contrast diagram of magnetic flux density in damping gap before and after optimizing

It can be seen from Fig. 8 that although the length of the damping gap of the adjacent exciting coil is reduced after optimization, the magnetic induction intensity in the damping gap is increased by about 19%, which is close to the saturated state. At the damping gap corresponding to the exciting coil, the magnetic induction strength before and after optimization is almost the same. The optimized damping torque of the magnetorheological damper roller is 168.7N.m, which is about 21.7% higher than that before optimization.

5. Conclusion

An innovative design of multi-stage coil magnetorheological damping drum, the design is perfectly compatible with the traditional structure of non-damping drum. In this process, we propose a unique magnetic circuit design method and torque model. For the magnetorheological damper roll with a diameter of 108 mm, we find that the optimum number of exciting coils is 5, and the maximum output damping torque is 138 N.m. It should be noted that the velocity of the belt has no significant effect on the output damping torque of the damper. In order to further improve the performance of the damping roller, we use genetic algorithm to optimize the design. After optimization, the damping torque is increased by about 21.7%, and the effect is remarkable. However, in practical application, when the damping bracket works for a long time, its temperature will increase, resulting in a corresponding increase in speed and excitation current. Although we can control the damping torque well, how to effectively control the uniformity of magnetic field intensity is still a problem to be studied in the future.

Acknowledgement

This work was financially supported by Science and Technology Development Program of Wei Fang City, Shandong Province(2022GX040,2022GX041).

R E F E R E N C E S

[1] *Sarkar C, Hirani H.,* Theoretical and experimental studies on a magnetorheological brake operating under compression plus shear mode. Smart Materials & Structures, 2013, 22(11): 5032.

[2] *Yun D, Koo J H.* Design and analysis of an MR rotary brake for self-regulating braking torques. Review of Scientific Instruments, 2017, 88(5): 127-130.

[3] *Li Q, Huang W, Chen L, Wu C, Duan Ronghua, Min Yong*, Mechanism of Power System Stabilizer Affecting Frequency Oscillation and Damping Analysis Method. Automation of Electric Power Systems: 1-7 [2019-12-02]
.http: //kns.cnki.net/kcms/detail/32.1180.TP.20190904.1457.004.html.

[4] *Zhao Q*., "Installation technology and technical requirements of mine belt conveyor", Machinery Management and Development, vol. 37, no. 10, 2022, 311-312+317.

[5] *Ye T, Wang Q, Zhang C,* "Research and Implementation of Visual Monitoring System for Belt Conveyor", Lifting and Transportation Machinery, vol. 19, 2022, 42-46.

[6] *Wang Z X , Pu J T ,* "Research on the Suspension Force Model for the Large-Air-Gap Permanent-Magnet Suspension Belt Conveyor", in: Institute of Electrical and Electronics Engineers. 2021 3rd International Conference on Applied Machine Learning: 3rd International Conference on Applied Machine Learning (ICAML), 23-25 July 2021, Changsha, China. 2021.356-361.

[7] *D. Tian*, "Deviation analysis of belt conveyor and application research of roller deviation correction". Mechanical Management Development, vol. 37, no. 6, 2022, 63-65.

[8] *Zhao J.* Study on damping idler of downward belt conveyor for mine. Mechanical management development, 2023, 38(08): 68-70. DOI: 10.16525/J. CNKI. CN14-1134/th.2023.08.029.

[9] *Zhao J, Meng W, Wang Y, etc*. Finite element analysis of adjustable permanent magnetic damping roller. Modern Manufacturing Engineering, 2022, (05): 68-71. DOI: 10.16731/J. CNKI. 1671-3133.2022.05.011.

[10] *Yan M.* Optimal design of electromagnetic actuator and experimental study on active vibration control of pipeline. Harbin Engineering University, 2022. DOI: 10.27060/d. CNKI. GHBCU. 2022.001269.

[11] *Wang Y H, Zhang L Y, Ju C.* Magnetic field analysis and damping moment study of permanent magnet damping device. Coal mining machinery, 2021, 42(06): 35-37. DOI: 10.13436/J. Mkjx. 202106012.

[12] *Wang Y*. Study on permanent magnetic damping idler of downward belt conveyor. Taiyuan University of Science and Technology, 2021. DOI: 10.27721/d. CNKI. GYZJC. 2021.000088.

[13] *Zhou L, Jia Z, Bai Chungang et al*. Noise mechanism analysis and noise reduction method. Coal mining machinery, 2021, 42(04): 80-83. DOI: 10.13436/J. Mkjx. 202104025.

[14] Study on performance characteristics of low noise idler of belt conveyor. Taiyuan University of Science and Technology, 2021. DOI: 10.27721/d. CNKI. GYZJC. 2021.000308.

[15] *Liu J.* Deviation analysis and structural optimization improvement of mining belt conveyor. Mechanical Management and Development, 2022, 37 (10): 223-224+227. doi: 10.16525/j.cnki.cn14-1134/th.2022.10.

[16] *Aring Zhang,* Coal mine belt conveyor fault analysis and countermeasures discussion. Machinery Management and Development, 2022, 37 (10): 313-314+317. doi: 10.16525/j.cnki.cn14-1134/th.2022.10.17

[17] *Gong, J. M., Yang, H., Lin, S. H., Li, R., Zivkovic, V.* Spatial filtering velocimetry for surface velocity measurement of granular flow. Powder Technology: An International Journal on the Science and Technology of Wet and Dry Particulate Systems, 2018, 32476-84.

[18] *Zhang Y.* Research on automatic speed regulation system of belt conveyor based on AI intelligent video recognition. Shandong Coal Science and Technology, 2022, 40(08): 192-195.

[19] Gunter Schulz, Dieter Bokelmann, Michael GroB. Monitoring by Measurement and Possibilities of Correction of a Belt Conveyor. Gluckauf, 2001, 137(7/8): 380-384.

[20] *Na M.* Research on upgrading of belt conveyor driving device in coal mine transportation system. Mechanical Management and Development, 2022, 37 (08): 159-160+163. doi: 10.16525/j.cnki.cn14-1134/th.2022.08

[21] *Saechua W, Sharma S, Nakawajana N, et al.* Integrating Vis-SWNIR spectrometer in a conveyor system for in-line measurement of dry matter content and soluble solids content of durian pulp. Postharvest Biology and Technology, 2021(181-): 181.

[22] *Nam T H , Ahn K K* . A new structure of a magnetorheological brake with the waveform boundary of a rotary disk. Smart Materials & Structures, 2009, 18(11):115029.

[23] *Yu J , Dong X , Wang W* . Prototype and test of a novel rotary magnetorheological damper based on helical flow. Smart Materials & Structures, 2016, 25(2):025006.

[24*] Nguyen Q H , Choi S B*., Optimal design of a novel hybrid MR brake for motorcycles considering axial and radial magnetic flux. Smart Materials & Structures, 2012, 21(5):55003-55012(10).

[25] *Choi S B , Sohn J W , Gang H G .,* An experimental study on torque characteristics of magnetorheological brake with modified magnetic core shape. Advances in Mechanical Engineering, 10, 1(2018-1-01), 2018, 10(1):168781401775222.

[26] Wu J , Li H , Jiang X , et al. Design, simulation and testing of a novel radial multi-pole multi-layer magnetorheological brake. Smart Materials & Structures, 2018, 27(2).

[27] *Chen Deming, Cai Qingge, Zhang Jinqiu et al.* Design and Simulation of Multi-plate Magneto-rheological Fluid Clutch. Journal of Academy of Armored Force Engineering, 2013, 27(6):26-30.

[28] *Wang D M , Hou Y F , Tian Z Z* . A novel high-torque magnetorheological brake with a water cooling method for heat dissipation. Smart Material Structures, 2013, 22(22):025019.

[29] *Jae-Haeng H, Mun-Kyeom K, Geun-Pyo P, et al*. A reliability-centered approach to an optimal maintenance strategy in transmission systems using a genetic algorithm. IEEE Transactions on Power Delivery, 2011, 26(4):26-37.

[30*] Hermano A C, M. T D M*. Using genetic algorithms for device modeling. IEEE Transactions on Magnetics, 2011, 47(5): 35-47.